Mater. Res. Soc. Symp. Proc. Vol. 841 © 2005 Materials Research Society R11.2.1

Modeling indentation in linear viscoelastic solids

Yang-Tse Cheng[1] and Che-Min Cheng[2]
[1]Materials and Processes Laboratory, General Motors Research and Development Center, Warren, Michigan, USA
[2]Institute of Mechanics, Chinese Academy of Sciences, Beijing, China

ABSTRACT

Using analytical and finite element modeling, we study conical indentation in linear viscoelastic solids and examine the relationship between initial unloading slope, contact depth, and viscoelastic properties. We will then discuss whether the Oliver-Pharr method for determining contact depth, originally proposed for indentation in elastic and elastic-plastic solids, is applicable to indentation in viscoelastic solids.

1. INTRODUCTION

Instrumented indentation is playing an increasing role in the study of small-scale mechanical behavior of "soft" matters, such as polymers, composites, biomaterials, and food products. Many of these materials exhibit viscoelastic behavior, especially at elevated temperatures. Modeling of indentation into viscoelastic solids thus forms the basis for analyzing indentation experiments in these materials. Theoretical studies of contacting linear viscoelastic bodies became active since the mid 1950s by the work of Lee [1], Radok [2], Lee and Radok [3], Hunter [4], Gramham [5, 6], Yang [7], and Ting [8, 9]. In recent years, a number of authors have extended the early work to the analysis of indentation measurements [10-15]. In this paper, we examine, through analytical and finite element modeling, the relationship between initial unloading slope, contact depth, and viscoelastic properties. We will then discuss whether the commonly used Oliver-Pharr method [16, 17] is applicable to indentation in viscoelastic solids.

2. ANALYTICAL RESULTS

We consider a rigid, smooth, and frictionless conical indenter with half-angle θ indenting a viscoelastic solid that can be described by the constitutive relationships between deviatoric stress and strain, s_{ij} and d_{ij}, and between dilatational stress and strain, σ_{ii} and ε_{ii}, as:

$$\begin{aligned} s_{ij}(t) &= 2\int_0^t G(t-\tau)\frac{\partial d_{ij}(\tau)}{\partial \tau}\,d\tau \\ \sigma_{ii}(t) &= 3\int_0^t K(t-\tau)\frac{\partial \varepsilon_{ii}(\tau)}{\partial \tau}\,d\tau \end{aligned}, \tag{1}$$

where $G(t)$ is the stress relaxation modulus in shear and $K(t)$ is the hydrostatic stress relaxation modulus. The time dependent Young's modulus and Poisson's ratio are then given by $E(t) = [9K(t)G(t)]/[3K(t)+G(t)]$ and $\nu(t) = [E(t)/2G(t)] - 1$, respectively. In this paper, we further assume that Poisson's ratio is time independent, which is possible if $K(t)$ and $G(t)$ have the same time dependence. Under these assumptions, the relationship between load, $F(t)$, and displacement, $h(t)$, are given by [18]:

$$F(t) = \frac{8\tan\theta}{\pi(1-\nu)}\int_0^t G(t-\tau)h(\tau)\frac{dh(\tau)}{d\tau}\,d\tau\,. \tag{2}$$

The load-displacement relationship can therefore be obtained if the viscoelastic properties of materials, $G(t)$ and ν, are known. Conversely, the viscoelastic properties may be obtained from measured $F(t)$ vs. $h(t)$ relations by solving an integral equation. Eq. (2) reduces to the well-known equation for conical indentation into purely elastic solids [19],

$$F(t)=\frac{4G\tan\theta}{\pi(1-\nu)}h^2, \quad (3)$$

where G and ν are the time-independent shear modulus and Poisson's ratio, respectively.

Eq. (2) is a special case of a more general expression derived first by Graham [5] and Ting [8]. They showed that Eq. (2) is valid for loading where the contact area is a monotonically increasing function of time. Under the same condition, the ratio of contact depth to indenter displacement is the same as that in the purely elastic case [5, 8],

$$\frac{h_c}{h}=\frac{2}{\pi}. \quad (4)$$

The equations for unloading where the contact area decreases monotonically have also been derived [5, 8], though they are considerably more complicated. As a result, a number of authors have proposed methods for deducing $G(t)$ from indentation loading curves using Eq. (2) without using the information contained in the indentation unloading curves [18]. However, we have recently shown [18] that Eqs. (2) and (4) can be used to evaluate the initial unloading slope of unloading curves. Suppose unloading takes place at $t=t_m+\Delta t$ with a constant unloading rate of $dh/dt|_{t_m^+}=-v_0$, we have, using Eqs. (2) and (4) for $0\le t\le t_m+\Delta t$ and $\Delta t\to 0$,

$$\left.\frac{dF}{dh}\right|_{h=h_m}=\frac{4\tan\theta}{1-\nu}[G(0)h_c(t_m^+)-\frac{2}{\pi v_0}\int_0^{t_m}\left.\frac{dG}{d\eta}\right|_{\eta=t_m-\tau}h(\tau)\frac{dh(\tau)}{d\tau}d\tau]. \quad (5)$$

Here, the use of Eq. (2) for analyzing initial unloading slope may be justified because the contact area has not yet decreased as $\Delta t\to 0$. The second term on the right-hand side of Eq. (5) is a function of loading history. When the second term is negligible compared to the first term, which can be achieved by using fast unloading (i.e., large v_0), the relationship between unloading slope and contact area, becomes identical to that for purely elastic contacts [16,19],

$$\left.\frac{dF}{dh}\right|_{h=h_m}=\frac{4G(0)\tan\theta}{1-\nu}h_c=\frac{2}{\sqrt{\pi}}\frac{E(0)}{1-\nu^2}\sqrt{A}, \quad (6)$$

where $A=\pi(h_c\tan\theta)^2$ is the contact area at time, t_m, when unloading takes place from h_m. Eq. (5) suggests that the initial unloading slopes converge when the unloading rate is sufficiently fast. Once this limiting case is reached, Eq. (6) can be used to determine the "instantaneous" moduli, $G(0)/(1-\nu)$ or $E(0)/(1-\nu^2)$, provided that the contact depth, h_c or area, A, is known as a function of $h_m=h(t_m)$. The latter condition is provided by Eq. (4).

The most widely used method for estimating the contact depth or area is the procedure proposed by Oliver and Pharr [16, 17]. Based on the results of Sneddon [19] on the shape of the surface outside the area of elastic contacts for an indenter of conical and paraboloid of revolution, Oliver and Pharr developed an expression for, h_c, at the indenter displacement, h_m,

$$h_c=h_m-\xi\frac{F_m}{(dF/dh)_m}, \quad (7)$$

where F_m and $(dF/dh)_m$ are the respective load and the initial slope of the unloading curve at the indenter displacement depth, h_m. The numerical value of ξ is $(2/\pi)(\pi-2)$ for conical indenter. Although Eq. (7) is derived from solutions to elastic contact problems, it has been used to estimate contact depth for indentation in elastic-plastic solids [16, 17] and viscoelastic solids [20]. In the following, we examine the conditions for using Eq. (6) and the applicability of Eq. (7) by analyzing the complete loading-unloading curves and contact depths.

3. NUMERICAL RESULTS

We consider a frictionless, rigid conical indenter of half angle $\theta = 70.3$ degrees indenting an isotropic linear viscoelastic solid. A three-parameter "standard" linear viscoelastic model is used to describe the shear and hydrostatic relaxation modulus (see Fig. 1):

$$\begin{aligned} G(t) &= G_1\left(1 - \frac{G_1}{G_1+G_2}\left(1-e^{-t/\tau_s}\right)\right) \\ K(t) &= K_1\left(1 - \frac{K_1}{K_1+K_2}\left(1-e^{-t/\tau_s}\right)\right), \end{aligned} \tag{8}$$

where the relaxation time $\tau_s = \eta/(G_1+G_2)$. Various parameters are given in Table 1.

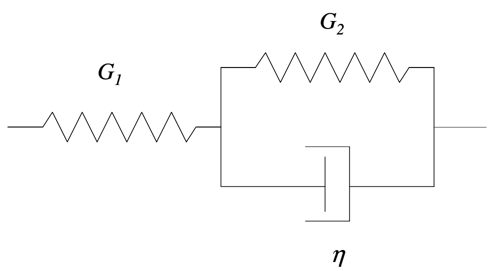

Fig. 1. *A three-parameter "standard" model for linear viscoelastic solids.*

G_1(MPa)	G_2(MPa)	K_1(MPa)	K_2(MPa)	τ_s(sec)
234.60	25.78	687.62	75.56	0.99

Table 1. *Parameters of a three-parameter linear viscoelastic model used for the calculations.*

The parameters are chosen such that Poisson's ratio is time independent, though both $G(t)$ and $K(t)$ are time dependent. Specifically, their values at $t = 0$ and $t = \infty$ are as follows: $G(0) = 234.60$ MPa and $G(\infty) = 23.23$ MPa ; $K(0) = 687.62$ MPa and $K(\infty) = 68.08$ MPa ; and $\nu = 0.4833$. The parameters of this fictitious model solid are used for illustration purposes. Because of linearity, the results can be scaled to represent other materials of the same general type when the dimensionless parameters, such as G_1/G_2, K_1/K_2, G_1/K_1, and t/τ_s, are equal. Finite element calculations were carried out using the classical isotropic linear viscoelastic model implemented in ABAQUS [21]. The finite element mesh is the same as that used in Ref. [22].

For the constant indentation displacement rate profiles given in Figure 2a, the corresponding loading-unloading curves from finite element calculations are shown in Figure 2b. Also shown in Fig. 2b are the initial unloading slopes. These examples clearly show that, for the same loading history, the initial unloading slopes converge when unloading rate is sufficiently fast, in agreement with Eq. (5). In fact, the complete unloading curve converges to one limiting case as the unloading rate increases. Consequently, we may define this unloading curve as the "converged" unloading curve for a given loading history.

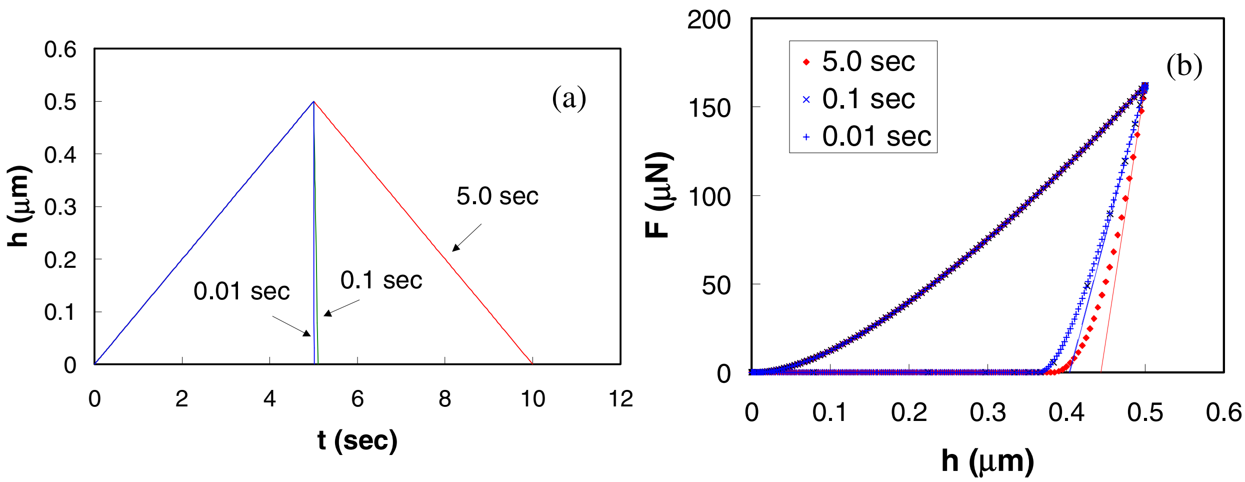

Fig. 2. *Displacement-time profiles (a) and the calculated loading-unloading curves (b) for the same loading rate and three different unloading rates. The tangent lines with initial unloading slopes are also shown (b). The loading-unloading curves are labeled by the time duration of unloading.*

The contact depth, h_c, and contact area, A, are also obtained from finite element calculations. The finite element results show that there is a small correction to Eq. (6),

$$\left.\frac{dF}{dh}\right|_{h=h_m} = \beta \frac{4G(0)\tan\theta}{1-\nu} h_c = \beta \frac{2}{\sqrt{\pi}} \frac{E(0)}{1-\nu^2} \sqrt{A}\,, \tag{9}$$

where $\beta = 1.05 \pm 0.02$. The same β correction factor has also been seen in the modeling of indentation in purely elastic solids and in elastic-plastic solids. The origin of this correction factor has been discussed previously [17, 18]. From finite element calculations, we found that $h_c / h \approx 0.658 \pm 0.001$, which is larger than $2/\pi \approx 0.636$ predicted by Eq. (4). This suggests that Eq. (4) needs to be slightly modified to become,

$$\frac{h_c}{h} = \alpha \frac{2}{\pi}\,, \tag{10}$$

where $\alpha = 1.034 \pm 0.001$.

Additional finite element calculations were carried out using constant indentation displacement rate profiles given in Fig. 3a. The loading curves in Fig. 3b show that the force required to reach a given indentation depth increases with the loading rate, consistent with the expected behavior of viscoelastic solids. The unloading rates chosen in the calculations are sufficiently fast so that they generate the corresponding converged unloading curves.

Furthermore, finite element calculations show that the contact depth, h_c, is the same for all three cases shown in Fig. 3b, as expected from Eq. (4) or Eq. (10) since h_m is the same. According to Eq. (9), therefore, the unloading slopes are the same, which is evident from Fig. 3b. These finite element results further validate Eqs. (9) and (10).

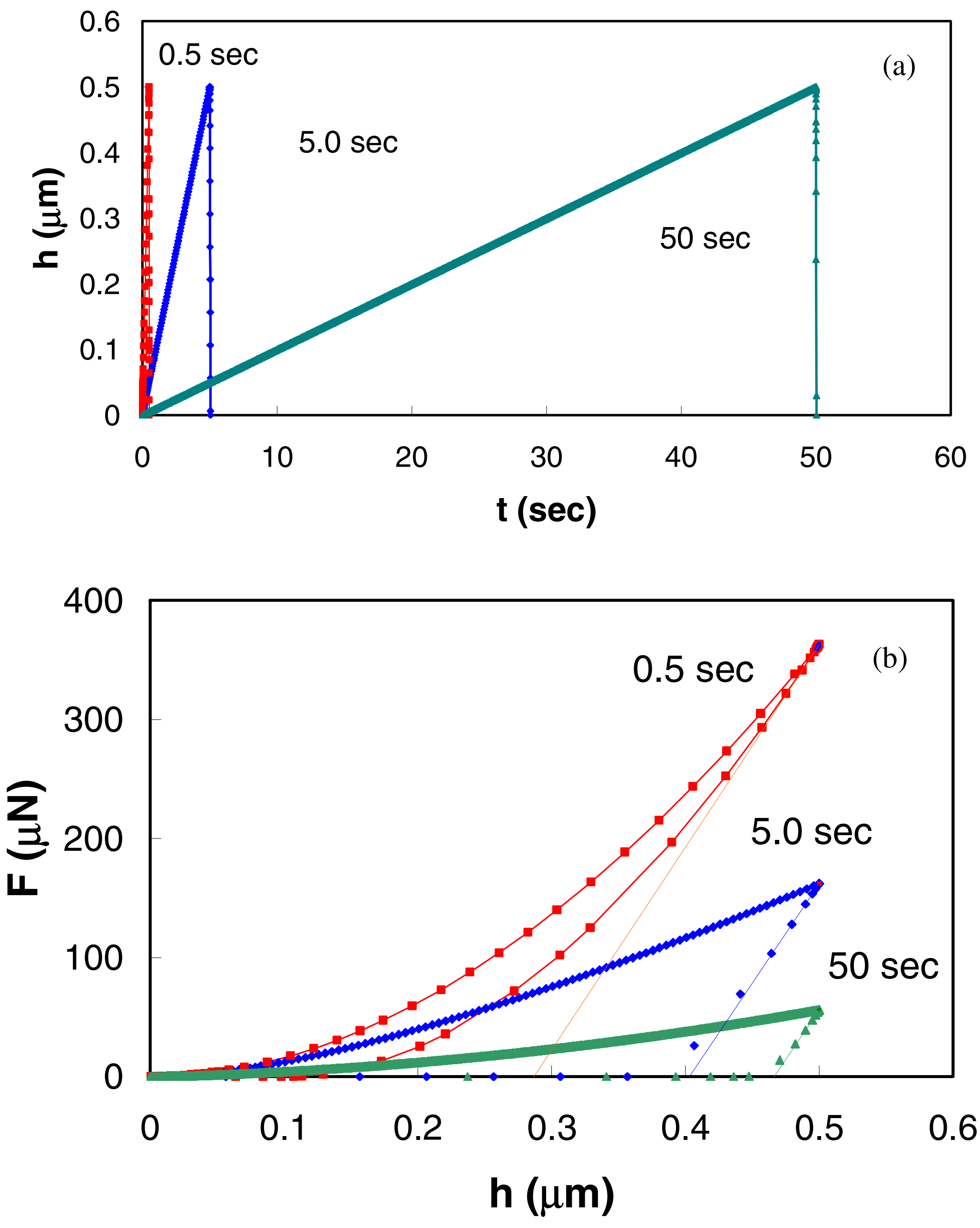

Fig. 3. *Displacement-time profiles (a) and the calculated loading-unloading curves (b) for three different loading rates and sufficiently fast unloading rates. The tangent lines with initial unloading slopes are also shown (b). The loading-unloading curves are labeled by the time duration of loading.*

On the other hand, Figure 3b demonstrates that the Oliver-Pharr procedure for estimating the contact depth, specifically Eq. (7), is not applicable to indentation in viscoelastic solids. This can be seen by the fact that Eq. (7) would have predicted different contact depths, h_c, since F_m is different while h_m and $(dF/dh)_m$ are the same for the three cases, contradicting the fact that h_c is the same. This observation is not surprising since Eq. (7) was derived from Eq. (6) which is only valid for conical indentation in purely elastic solids.

4. CONCLUSIONS

We have found that (1) a relationship, Eq. (9), between initial unloading slope, contact depth, and the instantaneous modulus for sufficiently high rate of unloading; (2) a relationship between contact depth and indenter displacement, Eq. (10); and (3) the Oliver-Pharr method for estimating the contact depth, Eq. (7), is not applicable to indentation in viscoelastic solids. Although these conclusions are based on the analysis of constant displacement rate loading conditions, the same conclusions hold for other loading conditions, such as constant loading-rate and constant indentation strain rate conditions.

ACKNOWLEDGEMENT

The authors would like to thank Wangyang Ni, Mike Lukitsch, Yue Qi, Tom Perry, and Wes Capehart, Lou Hector, and Mark W. Verbrugge for valuable discussions. C.-M. Cheng would like to acknowledge partial support from NSF of China, Project No.10372101.

REFERENCES

1. E. H. Lee, Quarterly Appl. Math. 13 (1955) 183.
2. J. R. M. Radok, Quarterly Appl. Math. 15 (1957) 198.
3. E. H. Lee, J. R. M. Radok, J. Appl. Mech. 27 (1960) 438.
4. S. C. Hunter, J. Mech. Phys. Solids 8 (1960) 219.
5. G. A. C. Graham, Int. J. Engng. Sci. 3 (1965) 27.
6. G. A. C. Graham, Int. J. Engng. Sci. 5 (1967) 495.
7. W. H. Yang, J. Appl. Mech. 33 (1966) 395.
8. T. C. T. Ting, J. Appl. Mech. 33 (1966) 845.
9. T. C. T. Ting, J. Appl. Mech. 35 (1968) 248.
10. L. Cheng, X. Xia, W. Yu, L. E. Scriven, W. W. Gerberich, J. Polymer Science: Part B: Polymer Physics 38 (2001) 10.
11. P.-L. Larrson, S. Carlsson, Polymer Testing 17 (1998) 49.
12. S. Shimizu, T. Yanagimoto, M. Sakai, J. Mat. Res. 14 (1999) 4075.
13. M. Sakai, S. Shimizu, J. Non-cryst. Solids 282 (2001) 236.
14. M. Sakai, Phil. Mag. A82 (2002) 1841.
15. M. L. Oyen, R. F. Cook, J. Mat. Res. 18 (2003) 139.
16 W. C. Oliver, G. M. Pharr, J. Mater. Res. 7 (1992) 1564.
17. W .C. Oliver, G.M. Pharr, J. Mat. Res. 19 (2004) 3.
18. Y.-T. Cheng and C.-M. Cheng, Mat. Sci. Eng. Reports: A Review Journal R44 (2004) 91.
19. I. N. Sneddon, Int. J. Eng. Sci. 3 (1965) 47.
20. For a review see: M. R. VanLandingham, J. Res. Nat. Inst. Stand. Tech. 108 (2003) 249.
21. HKS, Inc. (Pawtucket, Rhode Island 02860, USA).
22. W. Ni, Y.-T. Cheng, C.-M. Cheng, D. S. Grummon, J. Mat. Res. 19 (2004) 149.